Journal of Engineering Physics and Thermophysics, Vol. 74, No. 6, 2001

ESCAPE OF A RAREFIED GAS INTO VACUUM THROUGH A NONHOMOGENEOUS POROUS LAYER

E. Broverman,[a] **N. V. Pavlyukevich,**[b] **S. Rozin,**[a] **and Y. Ronen**[a]

UDC 533.7:536.423

Mass transfer in filtration or evaporation of a substance from a deepened surface in a highly porous layer and in escape into vacuum is calculated based on the Monte Carlo method. It is assumed that the porous layer contains individual inclusions in which the porosity is a random quantity. Account is taken of the possibility of the gas molecules being absorbed on the surface of the particles of the porous body. The angular distributions of molecules emerging from the layer are obtained. The nonmonotonic character of the distribution of the molecules absorbed which is caused by the presence of the inclusions is revealed.

Formulation of the Problem. As is well known [1], the microinhomogeneities of porous bodies which are caused by their chaotic structure and have a scale of about the pore size contribute to the additional transfer of heat and mass, which is reflected in the effective coefficients of transfer in porous media. However, in porous bodies there can be inhomogeneities caused by the irregular distribution of the porosity. Such inhomogeneities, whose scale is much larger than the scale of microinhomogeneities, can be considered to be random owing to the insufficient information on the structure of a porous medium, which leads to the irregularity of the average characteristics.

To solve problems in media with random inhomogeneities one sometimes employs approximate analytical methods [2, 3]. However, wider opportunities are opened up in the case of employment of numerical methods that are based on direct statistical modeling.

In the kinetic theory of gases, to describe the processes of transfer in highly porous homogeneous media one employs the dust-laden-gas model [4–6] in which the porous body is modeled by a homogeneous system of chaotically distributed stationary spherical particles of radius r. The mean free path of the gas molecules relative to the stationary particles of the porous body is determined by the expression

$$\lambda_\varepsilon = \frac{4}{3}\frac{\varepsilon}{1-\varepsilon} r\,, \tag{1}$$

while the number of these spheres in unit volume of the body with a porosity ε is equal to

$$n_\varepsilon = \frac{3\,(1-\varepsilon)}{4\pi r^3}\,. \tag{2}$$

In the present work, we calculated mass transfer in filtration or evaporation of a substance from a deepened surface in a model highly porous layer of thickness L_ε and escape into vacuum through the porous

[a]Ben-Gurion University, Be'ér Shevá, Israel; [b]Academic Scientific Complex "A. V. Luikov Heat and Mass Transfer Institute," National Academy of Sciences of Belarus, Minsk, Belarus. Translated from Inzhenerno-Fizicheskii Zhurnal, Vol. 74, No. 6, pp. 88–93, November–December, 2001. Original article submitted December 27, 2000.

1062-0125/01/7406-1475$25.00

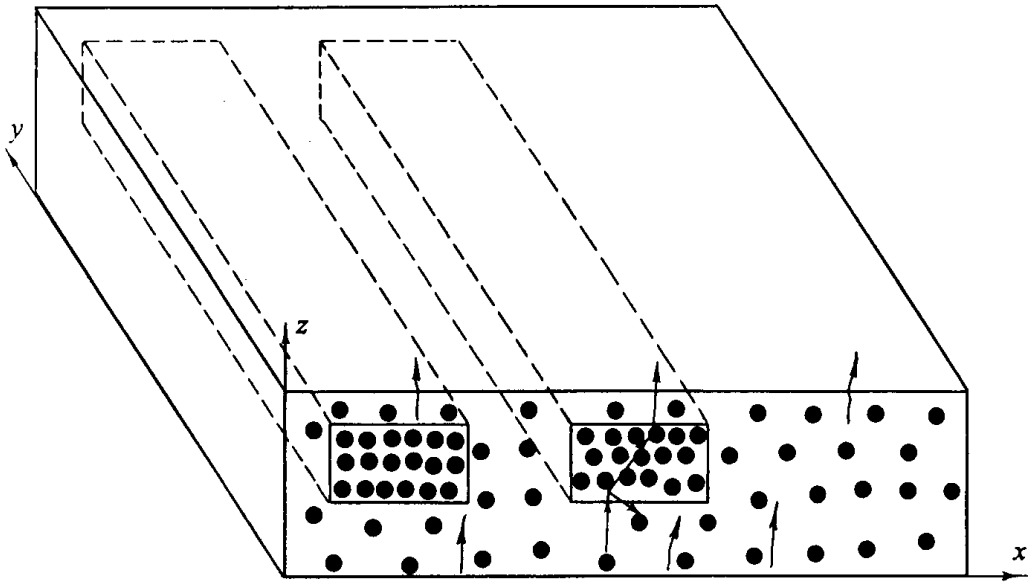

Fig. 1. Geometric scheme of the problem.

layer. Unlike [7], it is assumed that this layer is not homogeneous and contains individual inclusions in which the porosity (or the number of modeling spheres in unit volume) is a random quantity. We assume that the number of spheres K in unit volume of the inclusions obeys the discrete Poisson distribution [8]

$$P(K) = \frac{a^K}{K!} \exp(-a), \tag{3}$$

where $a = n_{\bar{\varepsilon}_i}$ is the average number of spheres in unit volume of the ith inclusion (mathematical expectation), which differs from n_ε of the basic mass. In this case, $n_{\bar{\varepsilon}_i}$ is related to $\bar{\varepsilon}_i$ by formula (2). The location and dimensions of the inclusions are considered to be prescribed here.

The thickness of the porous layer (Fig. 1) was taken to be equal to $L_\varepsilon = 5\lambda_0$ in the calculations. Two inclusions with dimensions $2 \times 10 \times 0.7$ cm each and a distance of 1 cm between them were located in the porous layer. Consideration was given to three positions of the inclusions over the layer height: the upper position from $z = 1.05$ cm to $z = 1.75$ cm, the lower position at the evaporation boundary $z = 0$, and the middle position. The inclusions were located along the x axis in the following manner: the first inclusion was located on the portion of the axis from $x = 1$ cm to $x = 3$ cm, while the second one was located on the portion from $x = 4$ cm to $x = 6$ cm. The porosity of the basic mass was $\varepsilon = 0.9$ and $r = 0.13\lambda_0$; the average porosity of the inclusions was $\bar{\varepsilon}_i = 0.7$–$0.98$. The calculated region had dimensions $10 \times 10 \times 1.75$ cm.

Method of Solution. *Free-molecular approximation (case 1).* It is taken that the gas and the skeleton of the porous body have the same temperature; the regime of one-component flow of the gas is assumed to be free-molecular (i.e., the gas molecules collide only with modeling spheres) and the law of reflection of the gas molecules from the spheres is assumed to be mirror or diffuse. From the deepened surface $z = 0$ the gas molecules arrive at the porous body (for example, filtration of the gas through the boundary $z = 0$ or evaporation of the substance from this surface).

The problem is solved by the Monte Carlo method in the mean-free-path approximation. The procedure begins by drawing the initial position of a "test particle" (a "beam" of actual molecules) on the deepened surface $z = 0$ in accordance with the law of a uniform distribution.

In this problem, for definiteness we will consider first the mass transfer through the porous layer of the molecules of the vapor of chromium in its evaporation from the surface $z = 0$ at $T = 1830$ K. The pressure of the saturated vapor p_e of chromium at this temperature is $p_e(T) \approx 0.1$ mm Hg ($\lambda_0 = 0.35$ cm), while the density of the flux I_{e0} of molecules evaporating from the surface is determined by the expression

$$I_{e0} = \frac{p_e(T)}{\sqrt{2\pi mkT}} = n_e \sqrt{\frac{kT}{2\pi m}} . \tag{4}$$

The test particles used in the numerical procedure are related to the flux of actual evaporating molecules in the following manner. If S is the area of the evaporation surface and 75,000 situations are drawn, this means that the small area S is subdivided into 75,000 cells; each cell will contain one test particle and it corresponds to $I_{e0}S/75{,}000$ actual molecules.

The initial direction of the test particle determined in relation to the normal at a point on the evaporation surface by the polar angle θ and the azimuthal angle φ is drawn from the diffuse law

$$\theta = \arcsin \sqrt{R_\theta} , \quad \varphi = 2\pi R_\varphi$$

(i.e., the distribution of the flux of emerging particles obeys the cosine law), where R_θ and R_φ are random numbers uniformly distributed on the interval [0, 1]. Thereafter the mean free path is drawn from the formula [8]

$$\lambda = -\lambda_\varepsilon \ln (1 - R_\lambda) , \tag{5}$$

here R_λ is a random number uniformly distributed on the interval [0, 1] and λ_ε is determined from (1); then the mirror (in this variant) reflection of the test particle from a sphere is drawn. If we arrive at any inclusion in the process of drawing of λ according to (5), the transition from the basic mass to the inclusion must be carried out with allowance for the dependence of λ_ε on the distance [8].

The number of spheres in the inclusions is drawn according to the Poisson formula (3). The drawing of each K (then $\varepsilon_K = 1 - \frac{4}{3}\pi r^3 K$) is followed by the drawing of $\lambda = -\lambda_K \ln (1 - R_\lambda)$, where $\lambda_K = \frac{4}{3}\frac{\varepsilon_K}{1 - \varepsilon_K} r$. We note that, according to the Poisson formula, the quantity a is equal to $\bar{n}_{\varepsilon_i}$ in each drawing of K.

Taking into account intermolecular collisions (case 2). From the above values of the initial data of the example in question and from the definition of the Knudsen number $\mathrm{Kn} = \lambda_0/\lambda_\varepsilon$. it follows that $\mathrm{Kn} \approx 0.64$. Therefore, strictly speaking, we must also take into account the collisions of molecules inside the porous body. As will be shown below, this is of particular importance in the problem with the absorption of the gas molecules inside the porous body.

In case 2, after drawing the initial position and direction of the test particle the magnitude of the mean free path is drawn from the following exponential law [7]:

$$\lambda = -\bar{\lambda} \ln (1 - R_\lambda) , \quad \text{where} \quad \frac{1}{\bar{\lambda}} = \frac{1}{\lambda_\varepsilon} + \frac{1}{\lambda_0} . \tag{6}$$

Expression (6) is used to determine a new position of the test particle, while the form of the process is drawn from the relation

$$w_\varepsilon = \frac{\bar{\lambda}}{\lambda_\varepsilon} = \frac{\lambda_0}{\lambda_0 + \lambda_\varepsilon} , \quad w_0 = 1 - w_\varepsilon , \tag{7}$$

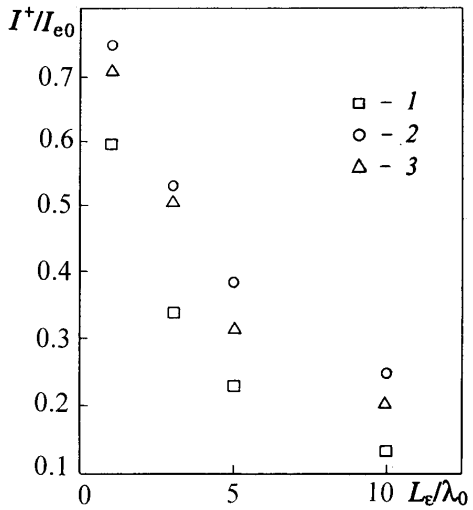

Fig. 2. Relative flux I^+/I_{e0} of the gas molecules emerging from a homogeneous porous layer vs. dimensionless thickness of the layer L_ε/λ_0: 1) free-molecular flow; 2) flow with account for intermolecular collisions; 3) data of [7].

where w_ε is the probability of collision of a molecule with a sphere and w_0 is the probability of collision of a molecule with a molecule. To take into account intermolecular collisions we employ the approximate procedure in accordance with which first consideration is given to free-molecular flow with allowance for the collisions of the test molecules just with the skeleton of the porous body. Then, in each spatial cell of the porous body, we determine the average direction of molecules passing through this cell (field distribution). At the next step, we already take into account the collisions of the molecules with each other; the direction of motion of a test molecule upon collision with a field molecule is determined in accordance with the law of elastic interaction. Next, if we arrive at an inclusion (with allowance for the dependence of λ on the distance), first the number of spheres in the inclusion is drawn according to the Poisson formula (3) and then the mean free path and the form of the process are drawn according to formulas (6) and (7) respectively (however, in (6) and (7) we use $\lambda_{\bar{\varepsilon}_i}$).

Absorption of the gas molecules. In this variant, we will consider that filtration occurs through a porous layer of rarefied gas whose molecules can enter into a heterogeneous reaction of first order on the surface of stationary spherical particles. By a heterogeneous reaction of first order we mean [6, 9] any process involving a solid surface which leads to a change in the important properties of molecules with a probability Ψ (for example, to a change in the chemical composition of a particle, the absorption of a particle by the wall, etc.). The molecules are mirror or diffusely reflected from the sphere surface with a probability $(1 - \Psi)$.

Discussion of the Results. Figure 2 gives the densities of unilateral fluxes of molecules I^+/I_{e0} emerging into vacuum through the surface of a uniform porous layer $z = L_\varepsilon$ as functions of the layer thickness. This relationship is determined by both the methods of kinetic theory [7] and the mean-free-path approximation which is used in this work. Consideration has been given to the above-mentioned variant of evaporation of a substance from the surface $z = 0$; therefore, the fluxes I^+ are referred to the quantity I_{e0} determined according to (10).

Comparison of our results in case 2 to the data of [7] shows that the employment of the approximate procedure for taking into account intermolecular collisions for Kn of about 1 is satisfactory, since the difference in the above-mentioned results is partially caused by the fact that we considered the mirror law of reflection of the molecules from the spheres while in [7] consideration has been given to the diffuse law of reflection.

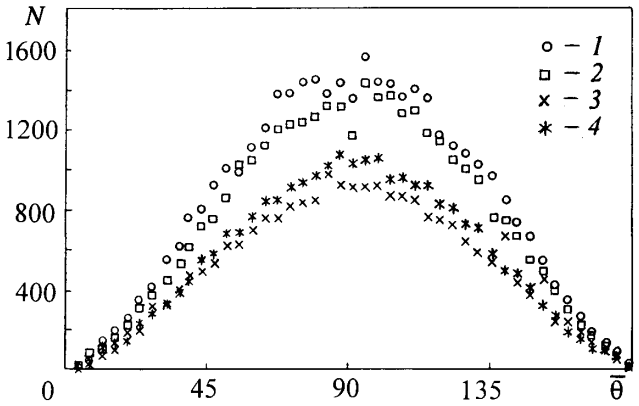

Fig. 3. Distribution of the number of test particles N emerging in the corresponding angular interval through the boundary $z = L_\varepsilon$ ($\bar{\varepsilon}_i = 0.7$): 1) homogeneous medium; 2) nonhomogeneous medium; 3) free-molecular flow in a homogeneous medium; 4) the same in a nonhomogeneous medium.

As is seen from Fig. 2, the molecular fluxes I^+/I_{e0} in case 2 are larger than the analogous quantities in case 1; in particular, for $L_\varepsilon/\lambda_0 = 5$ they are 1.6 times larger. This is attributed to the fact that in case 2 the appearing macroscopic velocity of ordered motion of the gas substantially increases the total molecular flux for the intense escape into vacuum in question.

Figure 3 presents the distribution of the number of test particles N emerging from a porous layer (both homogeneous and nonhomogeneous) at a certain angle $\bar{\theta}$ to the x axis (angular distributions). The total number of the situations drawn is 75,000.

It is of interest to note that in case 2 the distribution $N(\bar{\theta})$ in the homogeneous porous medium is more "complete" than in the nonhomogeneous layer. The reason is that in the flux with a macroscopic velocity of ordered motion (case 2) the velocities of a considerable part of the molecules are oriented in the direction of visible motion. The presence of inclusions denser than the basic mass ($\bar{\varepsilon}_i = 0.7$) at the upper boundary of the porous layer decreases the number of such molecules, since in these inclusions the Kn number increases (λ_ε decreases), i.e., the fraction of molecules colliding with solid spheres increases. For the same reason the influence of the macroscopic velocity on the total molecular flux decreases (as compared to the basic porous mass): the ratio of the total number of test molecules in case 2 ($\bar{N}_2$) to the analogous quantity in case 1 ($\bar{N}_1$) becomes equal to $\bar{N}_2/\bar{N}_1 \approx 1.3$, whereas for a homogeneous porous layer this ratio is equal to 1.6, as has been noted above.

It is noteworthy that the total number of molecules $\bar{N}$ emerging from the porous layer through the boundary $z = L_\varepsilon$ depends on the location of inclusions inside the layer. As the site of location of the inclusions with $\bar{\varepsilon}_i = 0.7$ is displaced from the surface $z = 0$ to the boundary $z = L_\varepsilon$ the quantity $\bar{N}$ increases. For the inclusions with $\bar{\varepsilon}_i = 0.98$ the situation is the reverse: $\bar{N}$ has the highest value when the inclusions are located at the boundary $z = 0$ and the lowest value in the case of location of the inclusions at the boundary $z = L_\varepsilon$. This is attributed to the fact that the denser inclusions at the boundary $z = 0$ reflect a smaller number of molecules back to the surface $z = 0$.

Also, of interest are the local angular distributions of molecules emerging from the boundary $z = L_\varepsilon$, for example, between the inclusions (Fig. 4) or over each inclusion. Figure 4 gives the distributions of the ratios γ of the number of molecules passed between the inclusions in the corresponding angular interval to the total number of molecules passed between the inclusions. It is seen from the figure that in the free-molecular approximation (case 1), a considerable scatter in values is observed in the angular distribution between

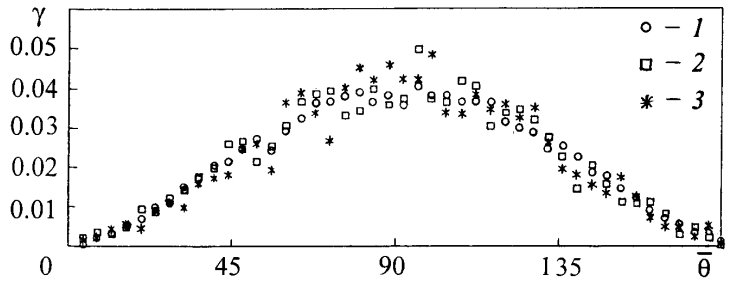

Fig. 4. Distributions of the ratios γ of the number of test particles emerging from the boundary $z = L_\varepsilon$ between the inclusions in the corresponding angular interval to the total number of molecules emerging between the inclusions ($\bar{\varepsilon}_i = 0.7$): 1) homogeneous medium; 2) nonhomogeneous medium; 3) free-molecular flow in a nonhomogeneous medium.

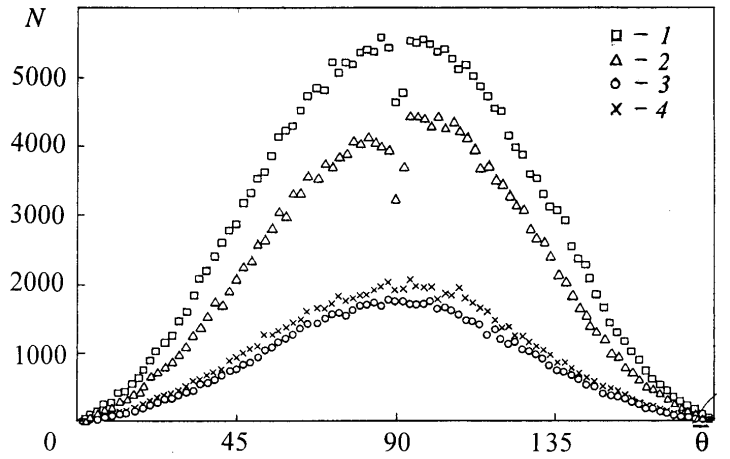

Fig. 5. Distributions of the number of test molecules N emerging in the corresponding angular interval through the entire boundary $z = L_\varepsilon$ in the presence of molecular absorption ($\bar{\varepsilon}_i = 0.7$, $\Psi = 0.2$): 1) homogeneous medium; 2) nonhomogeneous medium; 3) free-molecular flow in a homogeneous medium; 4) the same in a nonhomogeneous medium.

the inclusions, while taking into account the intermolecular collisions (case 2) significantly smooths out this distribution, bringing it closer to the corresponding curve for a homogeneous porous medium.

For the inclusions with $\bar{\varepsilon}_i = 0.98$ in case 1 we observe the "forward" extension in the local angular distributions owing to the presence of a part of the molecules emerging from the depth of the inclusions directly into vacuum without collisions with the spheres.

Thus, for the upper location of the inclusions the local angular distributions can differ from the angular distributions of molecules emerging through the entire boundary $z = L_\varepsilon$ from the entire porous layer.

Now we pass to the discussion of results of calculating the filtration of the gas into vacuum in the presence of a heterogeneous reaction of first order on the surface of the modeling spheres (absorption of the gas molecules). Since in the process in question the vanishing of particles occurs, the drawn number of situations was taken to be rather large (1 million.). Figure 5 gives the angular distributions of the number of test molecules N emerging through the boundary $z = L_\varepsilon$ from the entire porous layer in absorption of the molecules with $\Psi = 0.2$ in it and in the presence of inclusions denser than the basic mass ($\bar{\varepsilon}_i = 0.7$).

As is seen from Fig. 5, in the homogeneous porous medium, the difference in the numbers of molecules $\bar{N}$ passed through the porous layer in cases 1 and 2 is more considerable than in Fig. 4. This is attributed to the fact that in case 2, first, the macroscopic velocity of ordered motion of the gas occurs (as has

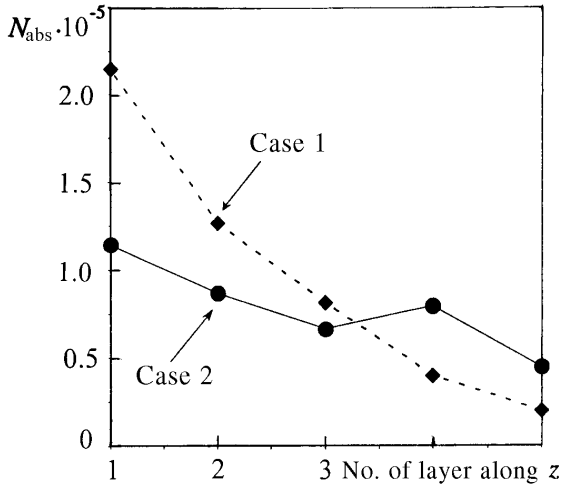

Fig. 6. Values of the numbers of absorbed test molecules N_{abs} in layers along the z direction ($\bar{\varepsilon}_i = 0.7$, $\Psi = 0.2$).

been noted above), which increases the resultant molecular flux and, second, in this case we have a decrease in the fraction of molecules colliding with the surface of the solid spheres and hence a decrease in the number of molecules absorbed. As a result, with molecular absorption ($\Psi = 0.2$), the ratio $\overline{N}_2/\overline{N}_1$ is approximately equal to 3.4, whereas without absorption ($\Psi = 0$) $\overline{N}_2/\overline{N}_1$ is approximately equal to 1.6.

In the presence of inclusions denser than the basic mass ($\bar{\varepsilon}_i = 0.7$), the ratio $\overline{N}_2/\overline{N}_1$ decreases and in the variant in question is equal to $\overline{N}_2/\overline{N}_1 \approx 2.2$ (for $\Psi = 0$, $\overline{N}_2/\overline{N}_1 \approx 1.3$). The reason is that the Kn number in such inclusions increases (λ_ε decreases), i.e., the fraction of molecules colliding with the solid spheres increases. Therefore, in the inclusions, more molecules are absorbed and the influence of the macroscopic velocity on the total molecular flux decreases (as compared to the basic mass).

If we compare the total molecular fluxes in case 1 for a homogeneous porous medium and a medium with inclusions, their difference is small, since the difference in the mechanism of absorption of the molecules in the inclusions and in the basic mass decreases significantly in the absence of the macroscopic velocity.

In the inclusions with $\bar{\varepsilon}_i = 0.98$, the Kn number decreases, i.e., the fraction of molecular collisions with the solid spheres decreases. Therefore, in the inclusions, fewer molecules are absorbed and more molecules are transmitted. Moreover, the macroscopic velocity in the total molecular flux is growing in importance.

Thus, in the problems of filtration of rarefied gases in porous media in the presence of heterogeneous physicochemical transformations in them, it is of prime importance to take into account intermolecular collisions even for rather high values of Kn (Kn ≈ 1).

Another important feature of the process in question is the nonmonotonicity of the distribution of the molecules absorbed over the porous body.

In particular, if the porous body in question is subdivided into five equally large layers along the z direction, we have the following distribution (Fig. 6).

The largest number of molecules (N_{abs}) is absorbed in the lower layers located near the particle source (the surface $z = 0$); with distance from the surface $z = 0$ the number of molecules absorbed decreases. However in case 2 in the upper layers with inclusions (the fourth and fifth layers), the situation is different: in the fourth layer, the number of absorbed molecules N_{abs} is even larger than the corresponding number in the third layer. Further, as the evaluations show, N_{abs} in the fourth and fifth layers in case 2 amounts to 33% and in case 1 to only 12% of the total number of molecules absorbed. This is attributed to the fact that, as has been noted above, in denser inclusions the Kn number increases and the fraction of molecules colliding

TABLE 1. Values of the Number of Absorbed Test Molecules N_{abs} in Layers along the x Direction

No. of layer along x	N_{abs}		No. of layer along x	N_{abs}	
	case 2	case 1		case 2	case 1
1	35881	50991	7	34243	49678
2	45830	46993	8	34327	49008
3	46301	46730	9	33840	48565
4	34025	49641	10	32765	45224
5	46365	47189	Σ	390164	480687
6	46587	47270			

with the solid spheres increases, i.e., the influence of the macroscopic velocity decreases (as compared to the basic mass) and the number of absorbed molecules increases. On the whole, the number of molecules absorbed in the porous body in case 2 is smaller than in the free-molecular case.

Table 1 gives the distribution of the absorbed molecules over ten layers which subdivide the porous body along the x direction; the first inclusion is located in layers 2–3, while the second inclusion is located in layers 5–6. We note that here we have the nonmonotonicity of the distribution of the absorbed molecules N_{abs} along the x axis in both case 2 and free-molecular case 1. In case 2, the number of molecules absorbed between the inclusions (and near them) is smaller than in the analogous volumes with inclusions. In the free-molecular case, the situation is the reverse: the number of molecules absorbed between the inclusions (and near them) is larger than in the analogous volumes with inclusions. The reason is the presence of numerous reflections of molecules from the denser inclusions and collisions of them with solid spheres beyond the inclusions.

More rarefied (than the basic mass) inclusions with $\bar{\varepsilon}_i = 0.98$ are also characterized by the presence of the nonmonotonicity of the distribution of absorbed molecules along the x axis. However here, unlike the variant with denser inclusions ($\bar{\varepsilon}_i = 0.7$), in cases 1 and 2 fewer molecules are absorbed in the inclusions than in the analogous volumes between the inclusion and near them. In case 2 this is related to a more substantial (than in the basic mass) influence of the macroscopic velocity on the total molecular flux in the inclusions, while in case 1 the reason is the emergence of molecules from the inclusions with their upper location without collisions.

Thus, we have revealed the nonmonotonicity of the distribution of absorbed molecules in a porous body, which points to the possibility of intensifying the physicochemical transformations and the processes of transfer in the vicinity of the inhomogeneities of a porous medium.

NOTATION

x, y, z, coordinate axes; ε, porosity; $\bar{\varepsilon}_i$, average value of the porosity in the ith inclusion; r, radius of the stationary spheres; n_ε, number of spheres in unit volume of the body with a porosity ε; L_ε, thickness of the porous layer; λ_ε, mean free path of the molecules relative to the stationary spheres; λ_0, gasdynamic free path of the molecules; Kn, Knudsen number; Ψ, absorption probability of the molecules; m, molecular mass; k, Boltzmann constant; $p_e(T)$, pressure of saturated vapor at T; I_{e0}, density of the flux of evaporating molecules; $N(\theta)$, number of test molecules emerging from the porous layer at an angle θ to the x axis; $\bar{N}$, number of test molecules emerging from the entire porous layer.

REFERENCES

1. L. I. Kheifets and A. V. Neimark, *Multiphase Processes in Porous Media* [in Russian], Moscow (1982).

2. Y. Ronen, *Kerntechnik*, **56**, No. 1, 47–48 (1991).
3. M. M. Shvidler, *Statistical Hydrodynamics of Porous Media* [in Russian], Moscow (1985).
4. E. A. Mason and A. P. Malinauskas, *Gas Transport in Porous Media: The Dusty-Gas Model* [Russian translation], Moscow (1986).
5. B. V. Deryagin and S. P. Bakanov, *Dokl. Akad. Nauk SSSR*, **115**, No. 2, 267–270 (1957).
6. N. V. Pavlyukevich, G. E. Gorelik, V. V. Levdanskii, V. G. Leitsina, and G. I. Rudin, *Physical Kinetics and Transfer Processes in Phase Transformations* [in Russian], Minsk (1980).
7. G. Gorelik, N. Pavlyukevich, S. Zalenskiy, S. Radev, and S. Stefanov, *Int. J. Heat Mass Transfer*, **36**, No. 13, 3369–3374 (1993).
8. N. P. Buslenko, D. I. Golenko, I. M. Sobol', V. G. Sragovich, and Yu. A. Shreider, *Method of Statistical Tests (Monte Carlo Method)* [in Russian], Moscow (1962).
9. A. I. Livshits, I. M. Metter, and L. É. Rikenglaz, *Zh. Tekh. Fiz.*, **16**, No. 2, 368–375 (1971).